

Performance and Design Concepts of a Free Electron Laser Operating in the X-ray Region*

Max Cornacchia for the LCLS Design Study Group[†]
Stanford Linear Accelerator Center, Stanford University, Stanford, CA 94309, USA[‡]

ABSTRACT

We report on the Design Study of a Free-Electron-Laser experiment designed to produce coherent radiation at the wavelength of 1.5 Å and longer. The proposed experiment utilizes 1/3 of the SLAC linac to accelerate electrons to 15 GeV. The high brightness electron beam interacts with the magnetic field of a long undulator and generates coherent radiation by self-amplified spontaneous emission (SASE). The projected output peak power is about 10 GW. The project presents several challenges in the realization of a high brightness electron beam, in the construction and tolerances of the undulator and in the transport of the x-ray radiation. The technical solutions adopted for the design are discussed. Numerical simulations are used to show the performance as a function of system parameters.

Presented at the Photonic West '97 Conference, San Jose, California, February 8-14, 1997.

* This work was supported by the Department of Energy Offices of Basic Energy Sciences and High Energy and Nuclear Physics, and Department of Energy Contract DE-AC03-76SF00515.

[†] *Stanford Linear Accelerator Center*: J. Arthur, K. Bane, V. Bharadwaj, G. Bowden, R. Boyce, R. Carr, W. Corbett, J. Clendenin, M. Cornacchia, T. Cremer, P. Emma, A. Fasso, A. Fischer, R. Gould, R. Hettel, J. Humphrey, D. Martin, B. McSwain, R. Miller, H.D. Nuhn, D. Palmer, M. Pietryka, S. Rokni, R. Ruland, J. Sheppard, R. Tatchyn, V. Vylet, D. Walz, H. Winick, M. Woodley, D. Yermian, R. Yotam. *European Synchrotron Radiation Facility*: A. Freund. *Lawrence Berkeley National Laboratory*: W. Fawley, K. Halbach, K.-J. Kim, S. Lidia, R. Schlueter, M. Xie. *University of California, Los Angeles*: C. Pellegrini. *University of Milan*: R. Bonifacio, L. De Salvo. *University of Rochester*: D. Meyerhofer.

[‡] Further author information - M.C., Stanford Linear Accelerator Center, M/S 69, P.O. Box 4349, Stanford, CA 94309, USA; Email: cornacchia@sslslac.stanford.edu; Telephone: 415-926-3906; Fax: 415-926-4100

1 Introduction

The SLAC linac presently accelerates electrons to 50 GeV for colliding beams experiments (the SLAC Linear Collider, SLC), and for nuclear physics experiments on fixed targets. In the near future, the first 2/3 of the 3 km linac will be used to inject electrons and positrons in the soon to be completed PEP-II B-Factory. The last 1/3 of the linac will be available for the production of an up to 15 GeV electron beam. The design discussed in this paper uses this electron beam to create a Free Electron Laser (FEL), the Linac Coherent Light Source (LCLS), capable of delivering coherent radiation of unprecedented characteristics at wavelengths as short as 1.5 Å. The LCLS is based on the Self-Amplified-Spontaneous-Emission (SASE) principle. The SASE mode of operation was first proposed¹ and analyzed for short wavelength FELs². In the SASE mode of operation high power, transversely coherent, electromagnetic radiation is produced from a single pass of a high peak current electron beam through a long undulator. SASE eliminates the need for optical cavities, which are difficult to build in the x-ray spectral region. However, the resulting requirements on the electron beam peak current, emittance and energy spread are very stringent and, until recently, difficult to achieve. The LCLS makes use of up-to-date technologies developed for the SLAC Linear Collider Project and the next generation of linear colliders, as well as the progress in the production of intense electron beams with radio-frequency photocathode guns. It is these advances in the creation, compression, transport and monitoring of bright electron beams that makes it possible to base the next (4th) generation of synchrotron radiation sources on linear accelerators rather than storage rings. These new sources will produce coherent radiation orders of magnitude greater in peak power and peak brightness than the present 3rd generation sources. Such a large increase in brightness, coupled with the very short pulse duration, will open new and exciting research possibilities in physics, biology and other sciences. The concept of an x-ray FEL based on the SLAC Linac and a photocathode injector³ was proposed in 1992^{4,5,6}. This proposal was followed by a period of studies⁷ until, in 1996, a Design Study was initiated that will form the basis of a formal construction proposal. This paper is a report of the work in progress.

2 Principle of operation

The FEL is based on the emission of radiation from relativistic electrons moving in an undulator magnetic field. The spontaneous radiation is emitted in a narrow line centered at the wavelength $\lambda = \lambda_u(1+K^2/2)/(2\gamma^2)$ where λ_u is the undulator period and K the undulator parameter⁸. The spectral width of the radiation line is related to the number of undulator periods, N_u , by $\Delta\omega/\omega = 1/(2N_u)$. In synchrotron radiation sources the spontaneous radiation is emitted incoherently, i.e. it arises out of random emission by the electrons with uncorrelated phases. This process is rather inefficient, and in fact, the intensity of the radiation is only linearly dependent on the number of electrons, N_e . If the electrons can be bunched in such a way that there is an appreciable component of the beam charge distribution function at the undulator frequency and the electron beam emittance is of the same order as the wavelength of the radiation, then the electrons emit coherently in the transverse direction and with coherence limited in time by the "spiking" effects that will be shown in Fig. 3.⁹ The intensity of the coherent radiation scales like the square of the number of electrons, a huge gain with respect to the incoherent emission. In an FEL operating under the Self-Amplified-Spontaneous-Emission principle, one or more electron bunches traverse the undulator once, and the build up of radiation occurs along the undulator. The electron beam interacts with the electric field of the radiation, that is perpendicular to the direction of propagation of the beam (the undulator axis), and parallel to the wiggling (transverse) velocity of the electrons produced by the undulator magnet, of amplitude K/γ ; the interaction produces an energy modulation at the scale λ . The electron energy modulation modifies the electron trajectory in the undulator in such a way as to produce bunching at the scale λ . Electrons bunched within a

wavelength all emit radiation that is in phase. The electromagnetic field creates more energy modulation and more bunching, leading to exponential growth of the radiation. The radiation is emitted in wave trains with a characteristic "cooperation length"⁹. For the SASE condition to be satisfied several basic conditions must be met^{1,10}:

- For the beam transverse emittances, $\varepsilon \approx \lambda/4\pi$.
- For the energy spread in a cooperation length (l_c), $\sigma_E/E < \rho$, where ρ is the FEL parameter $= [K\Omega_p f_B / (4\gamma\omega_u)]^{2/3}$, $\omega_u = 2\pi c/\lambda_u$ is the frequency associated to the undulator periodicity and $K = eB_u\lambda_u / (2\pi mc^2)$ (cgs units). $\Omega_p = (4\pi r_e c^2 n_e / \gamma)^{1/2}$ is the beam plasma frequency, n_e is the electron density, r_e is the classical electron radius and f_B is the Bessel function factor¹⁰. B_u is the undulator peak magnetic field, mc^2 the electron's rest energy. The cooperation length is $l_c = \lambda / (4\pi\rho)$.
- For the undulator length, $N_u\lambda_u \approx 10 L_g$, where L_g is the field gain length, $L_g \approx \lambda_u / (2\pi\sqrt{3}\rho)$.
- The radiation gain length must be shorter than the radiation Raleigh range, $L_g < L_R$, where $L_R = \pi w_0^2 / \lambda$ and w_0 is the radiation beam radius.

3 Overall layout

Fig.1 shows the layout of the proposed facility.

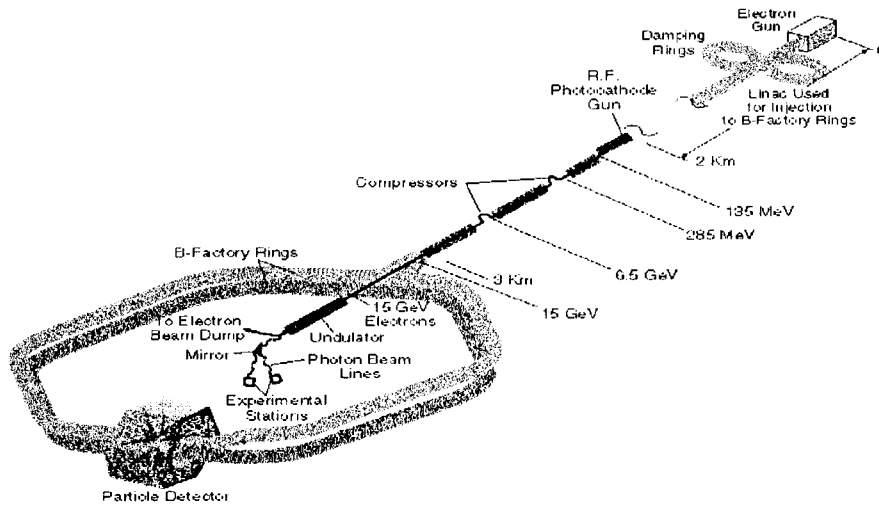


Figure 1: Layout of the Linac Coherent Light Source. Note the hexagonal shape of the soon to be completed PEP-II B-Factory electron-positron collider, that uses the first 2 km of the Linear Accelerator as the injector. The last one km of the Linac is used by the LCLS.

A new injector consisting of a gun and a short linac is used to inject an electron beam into the last kilometer of the SLAC Linac from where, after two stages of magnetic bunch compression, it emerges with the energy of 15 GeV, a peak current of 3,400 A and a normalized emittance of 1.5π mm-mrad. A transfer line takes the beam and matches it to the entrance of the undulator. The undulator, 100 m long, will be installed in the tunnel that presently houses the Final Focus Test Beam facility. After exiting the undulator the electron beam is deflected onto a beam dump, while the photon beam enters the experimental areas.

4 Performance characteristics

The following table lists some of the basic parameters of the LCLS electron beam, of the undulator and of the FEL performance.

Parameters		Units
Electron beam energy	14.35	GeV
Emittance	1.5	π mm mrad, rms
Peak current	3,400	A
Energy spread (uncorrelated)	0.02	%, rms
Energy spread (correlated)	0.10	%, rms
Bunch length	100	fsec, rms
Undulator period	3	cm
Number of undulator periods	3,330	
Undulator length	100	m
Undulator field	1.32	Tesla
Undulator gap	6	mm
Undulator parameter, K	3.7	
FEL parameter, ρ	$4.7 \cdot 10^{-4}$	
Gain length	11	m
Repetition rate	120	Hz
Saturation peak power	10	GW
Peak brightness	$5.5 \cdot 10^{32} - 5.5 \cdot 10^{33}$	Photons/(s mm ² mrad ² 0.1% BW)
Average brightness	$5.5 \cdot 10^{21} - 5.5 \cdot 10^{22}$	Photons/(s mm ² mrad ² 0.1% BW)

Fig. 2 shows the peak and average brightness as a function of photon energy.

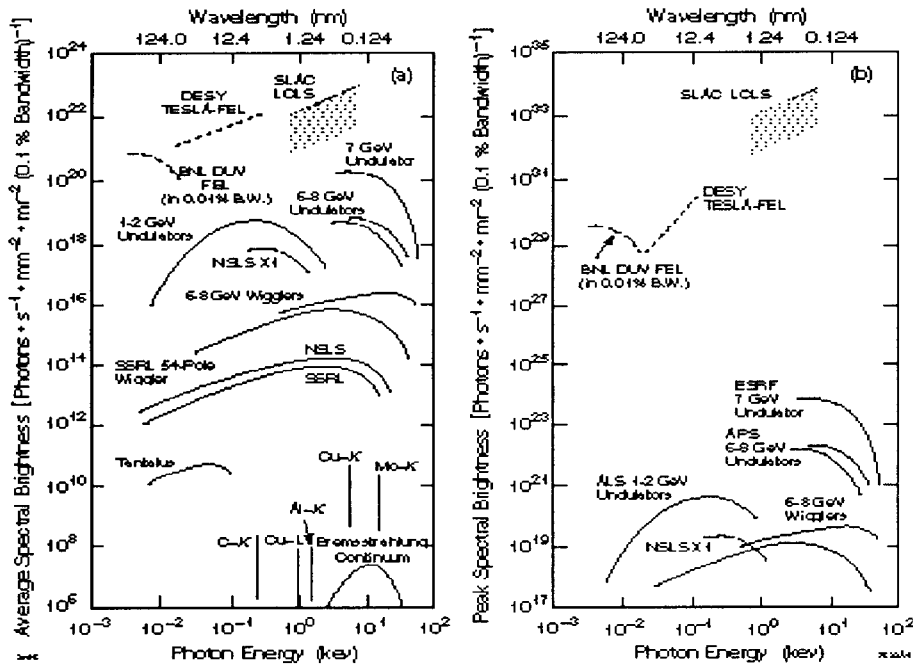


Figure 2: Average and peak brightness calculated for the LCLS, other planned FEL facilities and those obtained in some operating facilities.

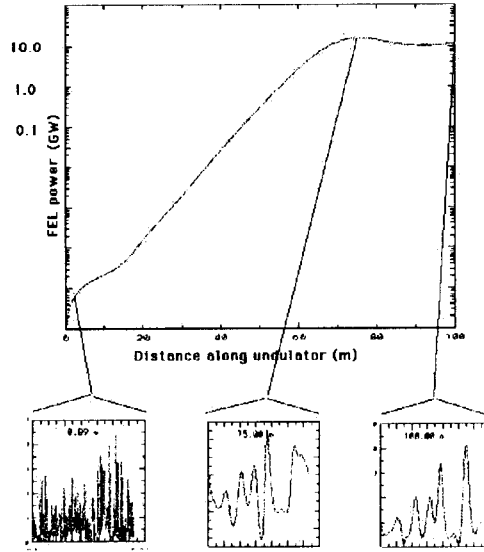


Figure 3: Build-up of the radiation power along the undulator length. The zoom on the microstructure shows the spiky nature of the radiation and the "clean-up" of the spectrum as saturation is approached.

The curves for the presently operating 3rd generation facilities indicate that the projected peak brightness of the LCLS would be about 8 orders of magnitude greater than currently achieved. Fig. 3 shows the build up of the FEL radiation along the undulator length, computed with the code "GIN-GER"¹¹. The power saturates, and reaches its maximum output value, at about 80 m along the undulator. A set of simulations takes into account the effect of magnetic imperfections.¹² This is shown in Figs. 4, where the length of undulator needed to reach saturation is plotted against the rms value of the dipole field errors in the magnetic poles of the undulator.

The simulation includes the correction of the electron beam trajectory with the correction system described in Section 7. The data points refer to rms errors in the detection electronics for the absolute position of the electron beam. This study indicates that the trajectory must not deviate from a straight line by more than 5-10 μm (i.e. a fraction of the 30 μm electron rms beam size) or else an appreciable reduction of FEL power ensues, due to imperfect overlap of the electrons with the radiation beam. Reduction in FEL power also occurs if the sequence of undulator poles is interrupted by a drift space. This phenomenon has been explained theoretically¹³, and it is mostly due to phase errors caused by the divergence of the beam as it drifts in free space. The impact of these considerations on the undulator design are discussed in Section 7.

5 The rf photocathode gun

The design goal of radio-frequency photocathode guns currently under development at various laboratories is an emittance of 1π mm-mrad (rms of the amplitude distribution) in an electron beam of 1 nC charge and there does not seem to be a fundamental limit to achieving 0.5π mm-mrad¹⁴. The LCLS design assumes a beam of rms emittance 1π mm-mrad containing 1 nC of charge and 3 ps long

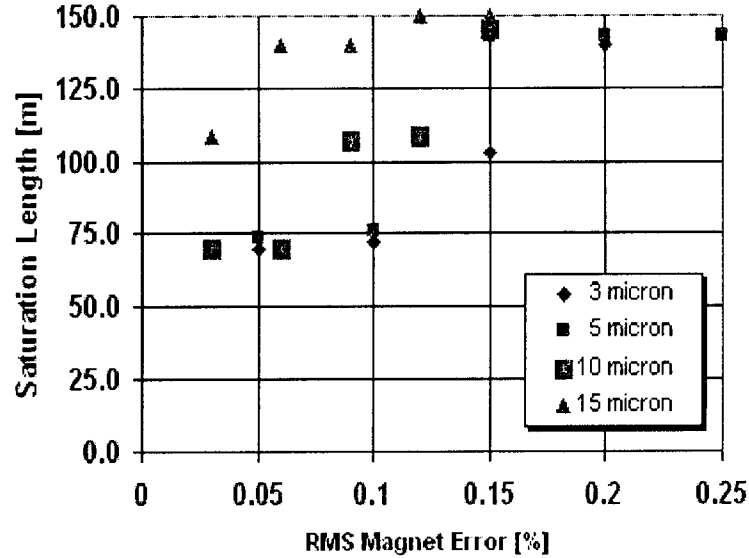


Figure 4: Undulator length needed to reach saturation as a function of the rms value of the dipole field errors in the undulator poles for various beam position monitor errors (3, 5, 10 and 15 microns)

(rms value).

In a radio-frequency photocathode gun, electrons are emitted by a laser beam striking the surface of a cathode³. The extracted electrons are accelerated rapidly (to 7 MeV) by the field of a radio-frequency cavity. The rapid acceleration reduces the increase in beam emittance that would be caused by the space charge field. The variation of phase space distribution along the bunch, caused by the varying transverse space charge field along the bunch, is compensated with an appropriate solenoidal focusing field¹⁵.

The laser will have a Nd:YLF- or YAG-pumped Ti:sapphire amplifier operating at 750 nm that will be frequency tripled (3rd harmonic). Very restrictive conditions are required for the reproducibility, from pulse-to-pulse, of the laser energy and timing. Stable FEL operation requires a pulse-to-pulse energy jitter of better than 1% and a pulse-to-pulse phase stability of better than 0.5 ps (rms). These tight stabilities are needed to ensure optimum compression conditions.

6 Compression and acceleration

The layouts of the accelerator and compression system are shown in Fig. 5.

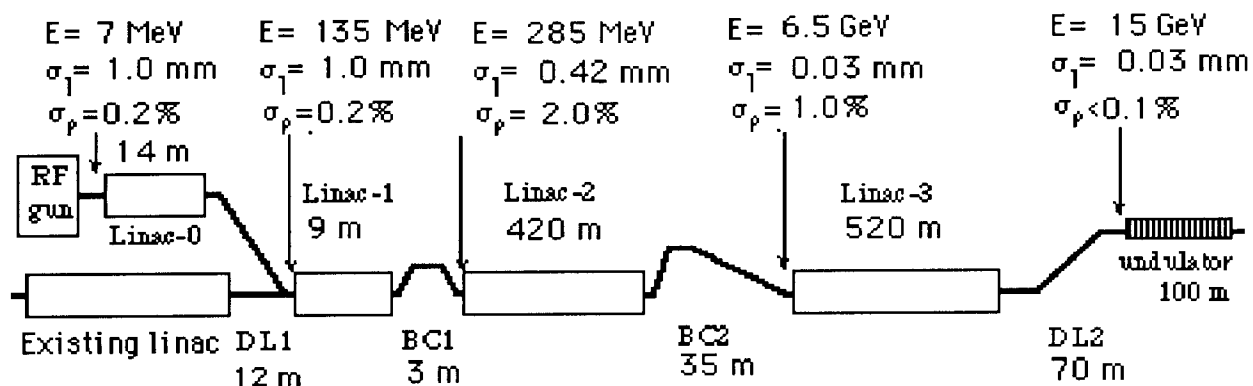


Figure 5: Layout of the acceleration and magnetic compression system.

The electron gun is displaced with respect to the Linac axis to allow a straight through beam from the first 2/3 of the linac to be accelerated to 50 GeV for other, non FEL related, applications. The purpose of the compressors is to reduce the bunch length and increase the peak current to the 3,400 A required to start the SASE process. Compression is achieved by creating an energy-phase correlation by accelerating the beam off crest in Linac-1, after which the chicanes shorten the bunch by appropriate energy-path length dependence. It is preferable to utilize two, rather than one, chicane. This reduces the sensitivity of the final bunch length to the phase jitter in the photocathode laser timing¹⁶. The rms length of the bunch emitted from the cathode is 1 mm (3 psec). After compression, the bunch shortens to 0.03 mm.

The choice of energies of the various compression stages is the result of an optimization that takes into account beam dynamics effects, the most relevant ones being the space charge forces in the early acceleration stage, the wakefields induced by the electromagnetic interaction of the beam with the linac structure¹⁷ and the coherent synchrotron radiation emitted by a short bunch¹⁸. The lower limit on the choice of the energy of Bunch Compressor 1 (BC1) is set by space charge forces where the bunch is shortest. The upper limit is set by the desire to initially compress the bunch early in the linac to ease transverse wakefields. The energy of BC2 is set by the requirement to produce a small energy spread at 15 GeV. This requires a balance between longitudinal wakefields in Linac-3 and the energy-phase correlation just after BC2. The wakefields in Linac-3 scale with linac length and simulations with BC2 at 6.5 GeV (described below) have produced the required beam conditions at 15 GeV. The second compressor (BC2) is asymmetric with the last two dipole having a weaker field to avoid the emittance blow up induced by the coherent synchrotron radiation emitted in the bends where the bunch is shortest. With all dynamic effects included, the simulations¹⁹ indicate that the emittance blow up at the entrance of the undulator should be less than 50%, most of which is due to the transverse wakefields in Linac-2.

A full simulation of the longitudinal beam dynamics from rf gun to end of Linac-3 has been computed²⁰, including non-linearities, longitudinal wakefields and sinusoidal rf curvature. The input beam was of Gaussian distribution cut at $\pm 2\sigma$ in energy and bunch length with a 1 mm rms length and 0.2% rms energy spread (after cuts) at 7 MeV and a bunch population of $6.3 \cdot 10^9$ electrons. Fig.6 shows the longitudinal phase space at the entrance and exits of the 1st and 2nd compressor.

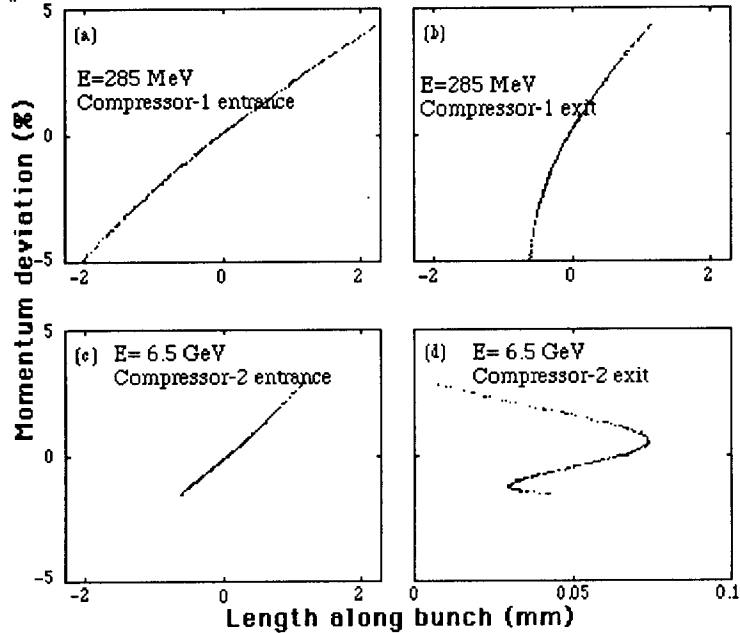


Figure 6: Longitudinal phase space distribution before and after compression.

The fwhm (full width half maximum) bunch length at 6.5 GeV is $44 \mu\text{m}$ with about 5kA of peak beam current. There are long tails on the energy distribution with a fwhm energy spread of 0.03 % where 75% of the particles are contained within a $\pm 0.15\%$ window.

From the Linac exit a transport system carries the beam to the entrance of the undulator.

7 The undulator

Several candidate undulator types were evaluated, including pure permanent magnet helical devices, superconducting bifilar solenoids and hybrid planar devices. Superconducting devices require more investment and resources than were available for this study, though they may offer a good solution. Permanent magnet helical devices offer a short gain length to reach saturation, but are built all around the beam pipe, making beam position monitors and vacuum design difficult. A planar undulator is more desirable, since it allows accessibility to the chamber and the magnetic measurement system is simpler than in a helical device, particularly in a small gap. Chamber accessibility is particularly important in this design, since, as mentioned earlier, theory¹³ and simulations indicate that a significant deterioration of performance occurs if the electron beam drifts in a free space for more than a few centimeters. This factor limits the interruption of the magnetic structure to insert quadrupoles, orbit correctors and beam position monitors. A planar pure permanent magnet undulator would allow the use of external magnets, but it would be considerably longer because of its lower field. A planar hybrid undulator (made of permanent magnets with iron poles) is preferable and was chosen on the ground of its shorter length, superior control of magnetic errors, and of the fact that the simulations have shown that the tunability that would be provided by external quadrupoles is not needed.

The electron beam is focussed by quadrupole fields obtained by shaping the ferromagnetic material

(vanadium-permendum) to provide a quadrupole field of 20 T/M in addition to the bending field of 1.32 T. The focusing structure is of the strong focusing F-D type, where F or D units are each 50 cm long. The matched β -function is 18 m. The focussing strength and period were chosen to minimize the loss of FEL power that occurs when the β -function difference between the F and D quadrupoles is too large. In our design the β -function beats by only a few percents.

The electron beam trajectory in the undulator requires periodic corrections to maintain overlap with the radiation field. Basically, the electron trajectory should be as close as possible to a straight line even in the presence of magnetic imperfections and misalignments. Since external correction is difficult in a hybrid design, the proposed correction method is to transversely move the focusing or defocusing blocks of the undulator poles to generate dipole steering fields. F and D units can be displaced by a maximum of $500 \mu\text{m}$ to deflect the beam by $100 \mu\text{rad}$. These displacements will be cam-actuated. The layout of the focussing and correction system is shown in Fig. 7.

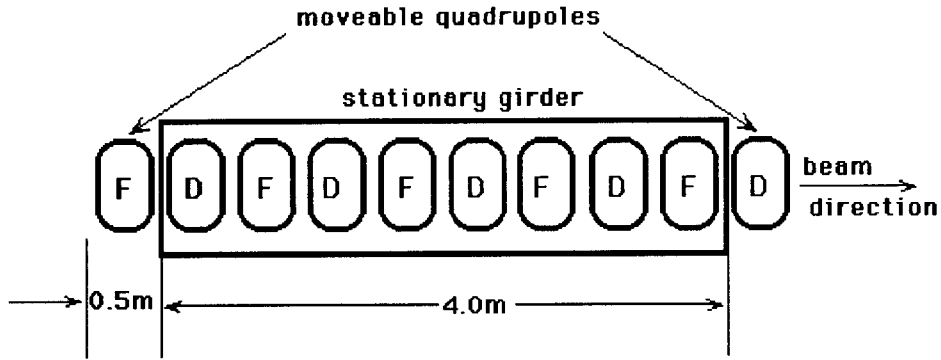


Figure 7: Diagram of the undulator focusing and trajectory correction system.

The simulations indicate that, with a pole-to-pole field reproducibility tolerance of 0.1%, if correction fields are spaced every 4.5 meters, the deviation of the electron beam trajectory can be held to less than $10 \mu\text{m}$. Fig. 8 shows the effectiveness of the proposed scheme to correct the orbit.

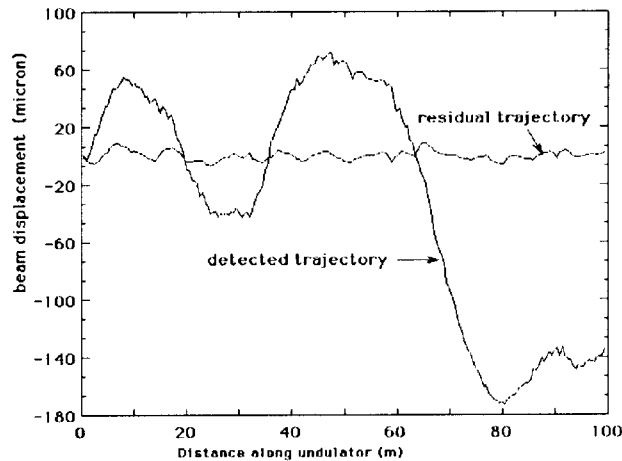


Figure 8: Electron trajectory in presence of undulator errors (large excursions) and after correction.

The "detected trajectory" is the uncorrected one as measured by a system of beam position monitors with their own detection errors ($2 \mu\text{m}$, rms, in measurement reproducibility); the "residual trajectory" is the one after correction, with a maximum deviation of the order of $10 \mu\text{m}$. The beampipe is constrained to have a very small vertical height, 6 mm, but its width can be large, 15 mm ID and 30 mm OD. The effect of the electron bunch striking the chamber has been calculated. If the grazing incidence strike angle is limited to no more than $150 \mu\text{rad}$ by a set of collimators upstream of the undulator, there is no serious puncture problem for aluminum or stainless steel beampipes for a single beam strike, though aluminum may suffer if the beam is parked on it for more than a few seconds. The present working assumption is of a stainless steel pipe with a 0.5 mm wall. Ion pumping will be used.

The undulator will be supported on piers spaced every 4.5 m, as shown in Fig. 9

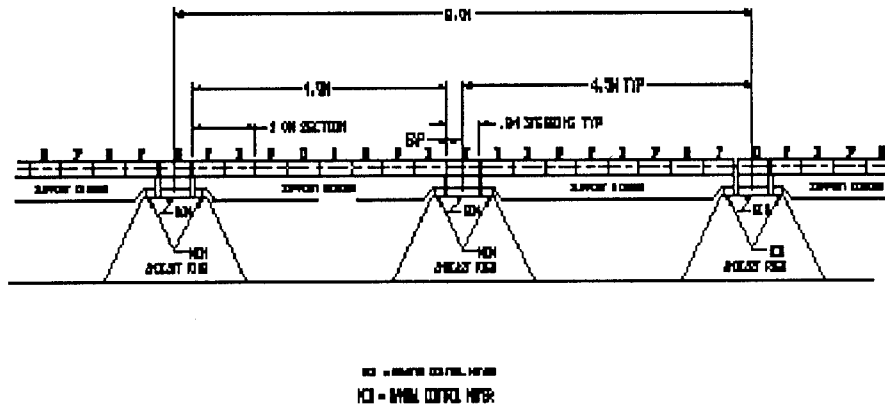


Figure 9: Undulator support system

Each support pier will be made of Anocast material which has a good long term stability and excellent damping ability. On top of each pier will sit adjustments to align each end of an undulator section and, in addition, to actively align the steering section. It is anticipated that the support sections and the undulator will be in a temperature stabilized enclosure independent of the shielding tunnel. This arrangement will prevent large temperature gradients across the supports and will maintain a constant temperature within ± 1 degree K.

A study of the radiation deposited in the undulator from beam-gas interaction revealed that the design is safe from long term damage to the magnetic material of the undulator. Collimators will be used to remove the beam halo.

8 Undulator alignment and beam monitoring

Fig. 4 indicates that the undulator length exceeds 100 m, a limit we have set, if the beam position monitors used to correct the orbit have detection errors greater than $5\text{-}10 \mu\text{m}$ with the expected rms pole-to-pole dipole field errors of 0.1%. The alignment and beam monitoring system is required to establish a straight trajectory to a tolerance of $5\text{-}10 \mu\text{m}$ over a length of approximately 10 m (one gain length) and to keep the trajectory from changing once it is established. Magnetic poles and beam position monitors have to be aligned to absolute and relative tolerances.

The tightest absolute tolerances are those of the individual F and D units ($5 \mu\text{m}$ rms). The

positioning tolerance of a F-D cell, and of a sequence of cells, is much more relaxed, 50 μm rms, because the kick of the F and D gradients nearly cancel each other. Conventional electromagnetic pick-ups normally do not guarantee an absolute determination of the position to better than 50 μm . On the other hand, these devices are excellent for measuring relative positions. Insertable carbon wires²¹ spaced at 4-5 m intervals will be used for absolute measurements of the beam position and for calibration of the adjacent stripline beam position monitors. Since these devices ultimately determine the limit to which the orbit can be corrected, they also have to be aligned to within the maximum allowed absolute orbit deviation (5-10 μm).

Achieving an absolute positioning tolerance of 5-10 μm is one of the challenges facing the LCLS where R&D effort will be required. Interferometric techniques^{22,23} seem to offer the best approach to this problem.

For relative positioning, a suspended wire system will be used. In this approach, a long wire is suspended in a pipe. Wire Position Monitors (WPM) measure the position of a wire excited with an AC signal²⁴. The WPMs are rigidly attached to the undulator magnets; if those magnets move with respect to the wire, the motion is detected by the WPM, fed back to the mover system, and corrected. The WPM has a readout resolution of 0.1 μm while the mover system, cam-based, is capable of a resolution of 0.5 μm . The mover system acts on the F and D elements depicted in Fig. 7 and labeled as "moveable quadrupoles".

9 The x-ray optics and experimental areas

After leaving the undulator, the electron beam, carrying a power of 1.8 kW, will be dumped into a shielding block by a sequence of downward-deflecting permanent magnets, while the FEL radiation will be transported downstream to the experimental areas. The design envisages the construction of 3 experimental hutches approximately 35 meters from the undulator exit, and one long beam line. To cover the full spectral range of the LCLS, both specular (1 hutch, for wavelengths longer than 4.5 \AA) and crystal (2 hutches, for wavelengths shorter than 4.5 \AA) optics will be employed. The peak power and power density of the radiation will be 6 orders of magnitude higher than anything currently handled by existing techniques, representing both an experimental challenge and a research opportunity. In initial operation it is expected that the high peak power and power density will inhibit the utilization of the full FEL flux with conventional focusing and transport optics. On the other hand, there will be a unique opportunity to study the effect of high peak power density on materials and optical elements, thereby opening the path to the full exploitation of the radiation in the LCLS and in future FEL facilities. We are consequently designing a system that will allow the intensity of the radiation to be varied from the level of current 3rd generation facilities up to the maximum LCLS intensity. This will be achieved by introducing a gas attenuation cell into the path of the FEL radiation. Such attenuation will, of course, reduce the LCLS brightness. For those experiments where the dilution in brightness is undesirable, the design incorporates a long (up to 700 m) beam line where the photon beam will be allowed to spread, reducing the power density on samples by up to a factor of 10^4 . Further reduction factors of 10^2 or more can be obtained on the beam line optics and instrumentation by operating their crystal or specular optical elements at very low grazing-incidence angles. Ultimately, by employing high-quality focusing optics at the exit of the long beam line, power densities many orders of magnitude higher than in the unfocused LCLS beam could also be attained, making the long beam line capable of providing a variation of 10 or more orders of magnitude in this parameter for a broad range of experimental applications.

10 Summary

We have described a layout of a proposed x-ray Free Electron Laser operating on the single pass SASE principle. The FEL uses the unique capability of the SLAC linear accelerator to create an intense electron beam of low emittance and a long undulator to produce high brightness coherent radiation down to about 1.5 Å. Theory and computations indicate that the peak brightness from such a device would be about 8 orders of magnitude greater than currently achieved in 3rd generation synchrotron radiation sources. Such performance, coupled with the very short bunch length (100 fsec rms) and full transverse coherence, would allow the exploration of new horizons in material science, structural biology and other disciplines.

11 REFERENCES

- [1] R. Bonifacio, C. Pellegrini, L.M Narducci, *Opt. Commun.* "Collective instabilities and high gain regime in a free electron laser", Vol. 50, No. 6 (1985); J.B. Murphy, C. Pellegrini, "Generation of high intensity coherent radiation in the soft x-ray and VUV regions", *Jour. Opt. Soc. of Ameri.* B2, 259 (1985).
- [2] K.-J.Kim, et al., "Issues in storage ring design for operation of high gain FELs", *Nucl. Instr. and Meth. in Phys. Res.* A239, 54 (1985); K.-J.Kim, "Three-dimensional analysis of coherent amplification and self-amplified spontaneous emission in free electron lasers", *Phys. Rev. Letters* Vol. 57, 1871 (1986); C. Pellegrini, "Progress towards a soft x-ray FEL", *Nucl. Instr. and Meth. in Phys. Res.* A272, 364 (1988).
- [3] R.L. Sheffield, "Photocathode rf guns", in *Physics of Particle Accelerators*, AIP Vol. 184, pp.1500-1531, M.Month and M.Dienes, eds., (1992).
- [4] C.Pellegrini, "A 4 to 0.1 nm FEL based on the SLAC linac", in *Workshop on Fourth Generation Light Sources*, SSRL Report 92/02, pp. 364-375, M. Cornacchia and H. Winick, eds., (1992).
- [5] K.-J. Kim, "Estimates of SASE power in the short wavelength region", *ibid.* pp. 315-324..
- [6] W. Barletta, A. Sessler and L. Yu, "Using the SLAC two-mile accelerator for powering an FEL", *ibid.*, pp. 376-384.
- [7] R. Tatchyn, J. Arthur, M. Baltay, K. Bane, R. Boyce, M. Cornacchia, T. Cremer, A. Fisher, S.-J. Hahn, M. Hernandez, G. Loew, R. Miller, W.R. Nelson, H.-D. Nuhn, D. Palmer, J. Paterson, T. Raubenheimer, J. Weaver, H. Wiedemann, H. Winick, C. Pellegrini, G. Travish, E.T. Scharlemann, S. Caspi, W. Fawley, K. Halbach, K.-J. Kim, R. Schlueter, M. Xie, D. Meyerhofer, R. Bonifacio, L. De Salvo, "Research and development toward a 4.5-1.5 Å Linac Coherent Light Source (LCLS) at SLAC", *Proc. of FEL95*, New York, NY 8/21-25/95; *Nucl. Instr. & Meth. in Phys. Res.*, A375 (1996) pp. 274-283.
- [8] See, for instance, P. Elleaume, "Free electron laser undulators, electron trajectories and spontaneous emission" in *Laser Handbook*, Vol. 6, pp. 91-114, W.B. Colson, C. Pellegrini and A. Renieri editors, North-Holland, 1990.
- [9] R. Bonifacio et al., "Spectrum, temporal structure and fluctuations in a high gain free electron laser starting from noise", *Phys. Rev. Lett.* 73, p.70 (1994).
- [10] J.B.Murphy and C.Pellegrini, "Introduction to the Physics of the Free Electron Laser", in *Laser Handbook*, Vol. 6, pp.9-70, W.B.Colson, C.Pellegrini and R.Ranieri eds., North-Holland, 1990.
- [11] Code written by W. Fawley.

- [12] The simulations have been done with the code FRED3D, written by T. Scharlemann.
- [13] K.-J. Kim and M. Xie, "Effect of wiggler interruption on LCLS performance", Lawrence Berkeley National Laboratory CBP Tech. Note-77.
- [14] R.L. Sheffield, "Working group II report: production and dynamics of high brightness beams", *Workshop on Nonlinear and Collective Effects in Beam Physics*, Arcidosso, Italy, Sept.2-6, 1996, proceedings to be published by the American Institute of Physics.
- [15] B. Carlsten, "New photoelectric injector design for the LOS Alamos National Laboratory XUV accelerator", *Nucl. Inst. and Meth. in Phys. Res.*, A285 (1989) 313.
- [16] T.O. Raubenheimer, "Electron beam acceleration and compression for short wavelength FELs", *Nucl. Instrum. Meth. in Phys. Res.* A358,40(1995)
- [17] See, for example, A. Chao, *Physics of Coherent Beam Instabilities in High Energy Accelerators*, Ch. 2, J. Wiley&Sons eds., New-York, 1993.
- [18] Ya. S. Derbenev et al., "Microbunch radiative head-tail interaction", DESY Report TESLA 95-05, Sept. 1995.
- [19] R. Assmann et al., "LIAR - A computer program for linear accelerator simulations", SLAC/AP-103, Oct. 1996.
- [20] Simulations done using the code "LITRACK", written by K. Bane.
- [21] C. Field, "The wire scanner system of the Final Focus Test Beam at SLAC", *Nucl. Inst. and Meth. in Phys. Res.*, pp. 467-475, A360 (1995).
- [22] "Vermessungsverfahren im Maschinen und Aulagenbau", Konrad Wittner Verlag, pp. 149 ff, Stuttgart, 1995.
- [23] L. Griffith, "The Poisson line as a straight line reference", *Proc. of 1st International Workshop on Accelerator Alignment*, p. 263 ff, SLAC Report 375, 1989.
- [24] R. Ruland et al., "A dynamic alignment system for the Final Focus Test Beam", in *Proceedings of the 3rd International Workshop on Accelerator Alignment*, Annecy, CERN, SLAC-Pub 6287, p. 243 ff., 1993.